HOSTED BY

Contents lists available at ScienceDirect

The Egyptian Journal of Remote Sensing and Space Sciences

journal homepage: www.sciencedirect.com

ELSEVIER

Research Paper

Assessment the Effect of Drought on Vegetation in Desert Area using Landsat Data ☆

H. Khosravi [a,*], E. Haydari [a], S. Shekoohizadegan [a], S. Zareie [b]

[a] Faculty of Natural Resources, University of Tehran, Iran
[b] Institute of Earth Sciences, Saint Petersburg State University, Saint Petersburg, Russian Federation

ABSTRACT

Drought phenomenon is one kind of a disaster that can significantly affect the density of vegetation in any area especially dry regions. This study tries to express the effect of drought on vegetation cover in Yazd-Ardakan plain, central Iran. At first, annual average for SPI index was calculated from 1996 to 2015, and then NDVI was calculated for May in 1998, 2000, 2009, 2010, 2011 and 2015. Afterwards, NDVI maps were classified into three groups including no vegetation, poor vegetation (pastures), and dense vegetation (farmlands and gardens). Based on the results the worst value of drought was −1.92 in year 1999. Besides, the annual SPI of 1996 with value of 2.4 was considered as the wettest year during study period (1996–2015). The highest percentage of dense vegetation and poor vegetation were related to 2010 and 1998 respectively, and the lowest percentage for both classes was related to 2000. There was correlation among the area of poor vegetation class in middle of spring and previous annual SPI at the significant level of 95%. In contract, no correlation was found between dense vegetation class areas in middle spring and previous amount of annual SPI. The study of the correlation between the SPI average and the percentage of vegetation classes indicated that pastures were highly sensitive to SPI changes; however, farming lands showed less sensitivity in short term due to using deep wells.

© 2016 National Authority for Remote Sensing and Space Sciences. Production and hosting by Elsevier B.V. This is an open access article under the CC BY-NC-ND license (http://creativecommons.org/licenses/by-nc-nd/4.0/).

1. Introduction

As an unpleasant climatic phenomenon that directly affects societies through the limiting access to water resources, drought is also followed by some huge economic, social and environmental costs (Goddard et al., 2003). This phenomenon is affected by rainfall, temperature, evaporation and transpiration, the content of humidity in accessible soil and the condition of underground water (Shahabfar et al., 2012; Montandon and Small, 2008).

Although meteorological information from ground stations has good accuracy and is popular worldwide, the distribution and density of meteorological stations is insufficient for the required spatial information detection (Brown et al., 2008; Unganai and Kogan, 1998; Skandari et al., 2016).

The spatial extent of drought cannot be properly identified unless there is a good distribution of meteorological stations throughout the area. Even then, the requirement of time and cost for the data preparation and chances of error, may hinder the procedures of drought mitigation. In this context, drought monitoring through satellite based information has been popularly accepted in recent years for its low cost, synoptic view, repetition of data acquisition and reliability (Dutta et al., 2015). In addition to the advantages mentioned, the Normalized Difference Vegetation Index (NDVI) and the Vegetation Condition Index (VCI) have been accepted globally for identifying agricultural drought in different regions with varying ecological conditions (Ji and Peter, 2003; Barati et al., 2011; Dutta et al., 2015). Satellite based NDVI is a useful tool for measuring and monitoring environmental conditions such as crop condition simulation, yield estimation, land degradation, dryland studies, etc. (Dutta et al., 2015; Aboelghar et al., 2010; Mondal et al., 2014; Boori et al., 2015).

Drought monitoring projects in USA are of the most interesting projects performed by some great organizations such as USDA, NDMC and NOAA in which drought has been studied across USA, and their up to date results are screened for the public access (Water and Become, 2005).

The research was conducted by Hadian et al. (2013) revealed that NDVI has a strong correlation with vegetation canopy. Therefore, using NDVI in monitoring vegetation cover and its relation to

meteorological parameters; in particular, precipitation might be applicable.

Ji and Peter (2003) carried out a study on vegetation response to accessible humidity by analyzing SPI and NDVI indices in the vast deserts in the north of America. This study was completed on grass vegetation and farming lands on the basis of three main goals including the study of the relation among Standardized Precipitation Index (SPI) and NDVI indices in various time scales, NDVI response to SPI in various periods of growing season and regional properties, and the relation between NDVI and SPI. They concluded that the best cohesion between NDVI and SPI was three months. Also, the best relation between SPI and NVDI in regions with low capacity in storing water was obtained in soil. Finally, the most important result was that NDVI is an effective index of humidity-vegetation condition, but for monitoring drought with NDVI index, seasonal scheduling should be also taken into consideration.

Yingxin et al. (2007) represented that there was a strong relationship among NDVI, NDWI and drought conditions by analyzing NDVI and NDWI collected from 5-years images of MODIC sensor for assessing drought in meadow of the great plain of America. Bhuiyan et al. (2006) monitored drought dynamism in Arawali in India by applying some meteorological indices and some indices obtained from satellite sensors, from 1984 to 2003. In their study, they utilized the SPI index for determining the rainfall deficit amount and the standardized water level index for assessing shortcoming and drainage of the underground water. Rahimzadeh et al. (2008) studied the possibility of using NDVI and VCI indices, extracted from AVHRR sensor of NOAA satellite, for monitoring drought in west north of Iran. They obtained the best cohesion between NDVI and VCI by 3-month rainfall (current month plus the past months), and in comparison with VCI, they found a better conformity between the NDVI and the rainfall.
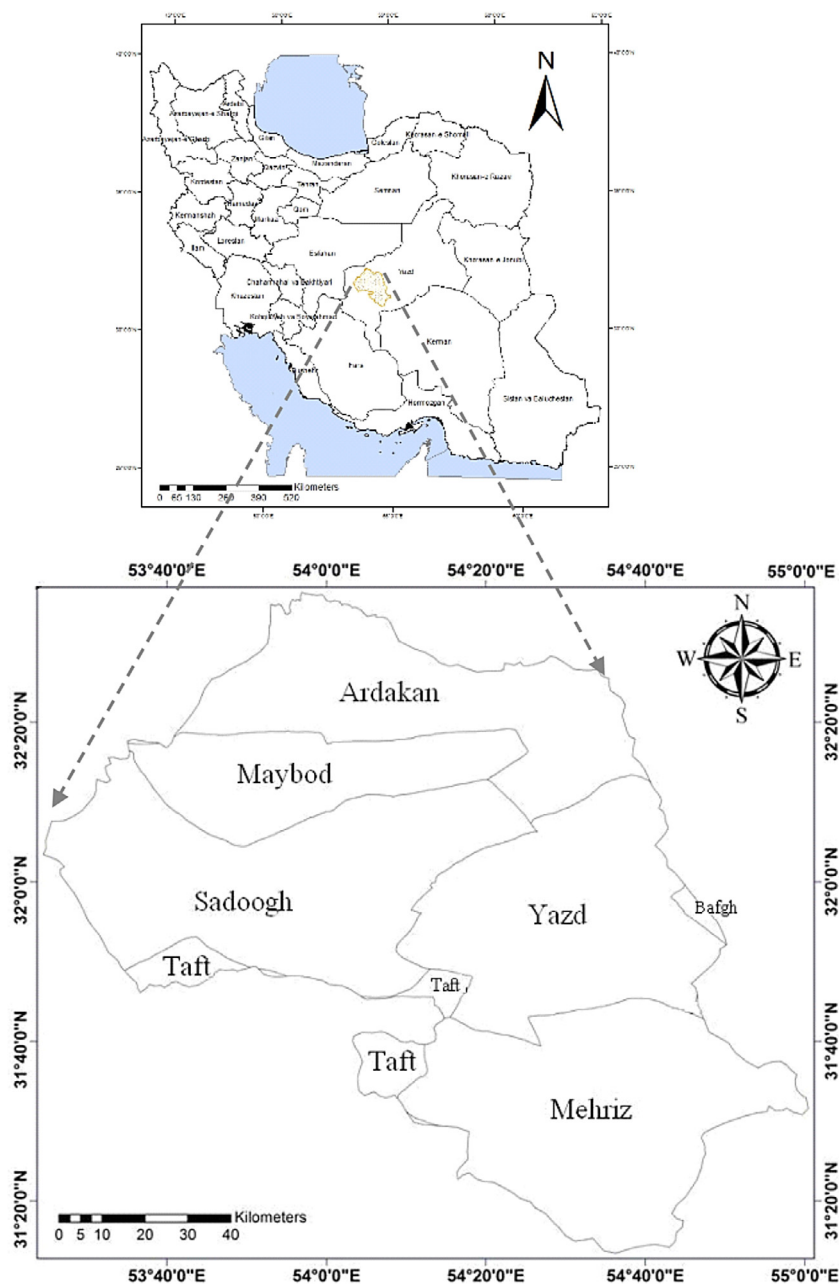

Fig. 1. The location of the study area.

Bevan et al. (2014) used NDVI regarding to changes in height in order to verify the response of plants to drought in 2003 in Europe. Jain et al. (2010) performed a study on the relationship between SPI in time scale of 1, 2, 3, 6, 9 and 12 months with NDVI, VCI and WSVI indices resulting from NOAA and AVHRR sensors in three states of India. After establishing cohesion relations among such indices in study areas, they concluded that the speed of vegetation reaction to drought changes is different in various areas. In a research at Australia, the relation between SPI and NDVI was studied in three time intervals of one, three and six months. The results revealed that the most cohesion coefficient was between the six-month SPI and NDVI (Caccamo et al., 2011); while the results of the same study in America indicated that it was between the three-month SPI and NDVI (Ji and Peter, 2003). It seems that the properties of vegetation, period of study, soil properties and dispersion and intensity of rainfall are important factors that can effect on the occurrence of the most cohesion coefficient between NDVI and the delay period of SPI (Moreira et al., 2008). Results of the research completed by Yazdanpanah et al. pointed out that the 6 to 12-month SPI index has the most cohesion with NDVI index (Yazdanpanah et al., 2014).

Alshaikh (2015) conducted a study to monitor and assess the drought condition in Wadi-Dama, north KSA, in 1990 and 2013 using satellite remote sensing data analysis and GIS technology. The results represented that the space technology application is one of the most important methods for the drought assessment, and also, remote sensing indices are the most effective means to detect and monitor the earth surface globally.

Dutta et al. (2015) attempted to identify the spatio-temporal extent of the agricultural drought over Rajasthan using remote sensing based Vegetation Condition Index (VCI), and assessed the performance of VCI by comparing the estimates with the meteorological drought indicator SPI, RAI and yield based the YAI index. They found that NOAA-AVHRR NDVI which derived VCI estimates, can be useful for monitoring the onset, the duration and the spatio-temporal extent of the agricultural drought. The study also proves and justifies the usefulness of remote sensing and GIS technique
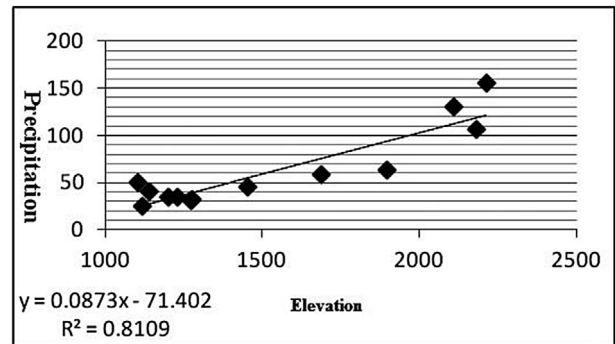

Fig. 3. The elevation-precipitation diagram of 1996.

for identifying the drought related stress in rain-fed crops. Unlike the meteorological data available in sparsely distributed meteorological stations, remote sensing based index VCI can be successfully used for delineating the spatio-temporal extent of agricultural drought.

The purpose of this research is to classify the NDVI index of Yazd-Ardakan plain, and also to compare the cohesion of these classes of area with SPI index for determining areas in which vegetation shows a quick reaction to drought in Yazd-Ardakan plain.

2. Materials and methods

2.1. Study area

Yazd-Ardakan plain is a part of catchment area of Siahkouh desert which is located in 53° 45′–54° 50′ eastern longitudes and 31° 15′–32° 30′ northern latitudes, almost in the center of Yazd province (Fig. 1). The area of this region is 11775 Square kilometers. The climate of this region is in type of desert dry with annual average rainfall of 61 mm according to 18-years data. The scope of this alluvial plain starts form foothill of Shirkouh (in the south),
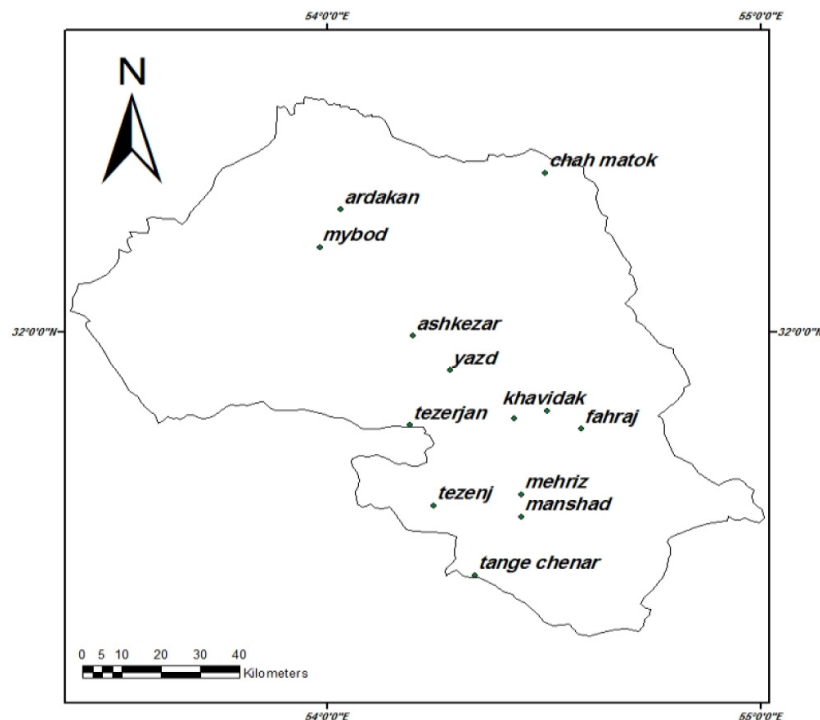

Fig. 2. The location of the concerned meteorological stations.

Table 1
SPI index Classes.

Class	SPI	Class	SPI
Slight drought	−0.8 to −0.5	Exceptional wet condition	>2
Medium drought	−1.3 to −0.8	Too severe wet condition	1.6–2
Severe drought	−1.6 to −1.3	Severe wet condition	1.3–1.6
Too severe drought	−2.8 to −1.6	Medium wet condition	0.8–1.3
Exceptional (acute) drought	< −2	Slight normal	0.5–0.8
–	–	Normal	−0.5 to 0.5

and it continues with a moderate gradient and in a valley like bedding up to Siahkouh desert (in the north) over 120 km.

2.2. Methodology

2.2.1. Calculation of SPI average

The SPI that is accepted by the world climatic organization as a reference drought index for the describing drought (Potop et al., 2012) which is obtained from the Eq. (1):

$$\text{SPI} = \frac{Pi - \bar{P}}{S} \qquad S = \sqrt{\frac{\sum_{1}^{i}(Pi - \bar{P})^2}{n}} \qquad (1)$$

where

    Pi = the Rainfall of the given period
    S = the Standard deviation
    P = the average of the Period of the rainfall
    N = the Number of data in a single period

Negative values of SPI index indicate drought, but the severity of the drought and its classification in different resources can be defined by considering conditions of that region in an optional way. The studies indicate that it's better to consider −0.5 as the beginning of the drought in Iran (Hamedan Province Meteorological General Department website: www.sinamet.ir). For calculating this index, at first, by assessment of pluviometry stations information existing in study area, rainfall data of 13 stations were selected from April 1996 to March 2015. The dispersal of stations is shown in Fig. 2.

In this research, for calculating the annual SPI index at first, rainfall map for each period was obtained in ArcGIS9.3. For this purpose, a diagram for the height-rainfall for each period was drawn by using height of meteorological stations and the amount of rainfall. Then by utilizing this diagram, the relation between the height and the rainfall was obtained for each period. In Fig. 3, the diagram is mentioned as an example for the height-rainfall in 1996.

Afterward, in ArcGIS9.3, height was replaced with DEM map (Digital Evaluation Model) with 30 m precision in this relationship, and the rainfall map for each period was obtained. As the next step in ArcGIS9.3, the map of the period's rainfall average and the period's standard deviation were obtained by employing Eq. (1). After this stage, the obtained map from the minus of rainfall map for each period to the rainfall average map for total period was divided to period standard deviation map. As a result, SPI map for the given period was obtained. In the next stage, maps for SPI index were classified by using Table 1 in which the numerical domain for various classes for that index was inserted. It should be noted that for highlighting droughts, the number of SPI classes has increased comparing to other studies.

2.2.2. Utilized satellite sensors

Multispectral Landsat TM and OLI images were used for obtaining vegetation indices. Properties of TM and OLI sensor are given in

Table 2
Spectral properties of Landsat TM and OLI sensors.

Name of satellite	Sensor	Band No.	Band spectral domain (micrometer)	Name of spectral domain	Resolution (meter)	Coverage dimensions (km)
LANDSAT	TM	1	0.45–0.52	Blue	30	185 × 185
		2	0.52–0.60	Green	30	
		3	0.63–0.69	Red	30	
		4	0.76–0.90	NIR Infrared	30	
		5	1.55–1.75	Middle infrared	30	
		6	10.4–12.50	Thermal Infrared	120	
		7	2.08–2.35	Middle Infrared	30	
	8-OLI	1	0.43–0.45	Coastal	30	
		2	0.45–0.51	Blue	30	
		3	0.53–0.59	Green	30	
		4	0.64–0.67	Red	30	
		5	0.85–0.88	NIR	30	
		6	1.57–1.65	SWIR 1	30	
		7	2.11–2.29	SWIR 2	30	
		8	0.50–0.68	Pan	15	
		9	1.36–1.38	Cirrus	30	
		10	10.60–11.19	TIRS 1	30 (100)	
		11	11.50–12.51	TIRS 2	30 (100)	

Table 3
The average of SPI in years of study.

Year	Annual SPI	Year	Annual SPI	Year	Annual SPI	Year	Annual SPI	Year	Annual SPI
1996	−0.79	2000	−0.36	2004	0.4	2008	−0.74	2012	0.52
1997	0.35	2001	0.49	2005	−0.76	2009	0.35	2013	0.48
1998	2.4	2002	1.16	2006	0.39	2010	−0.82	2014	−0.23
1999	−1.92	2003	0.77	2007	−0.31	2011	−0.64	2015	−0.45

Table 2. These images relate to 1998, 2000, 2009, 2010, 2011 and 2015. Also, the images have been registered every year in May.

2.2.3. Pre-processing of satellite data

Raw images of remote sensing always have some errors in geometry and registered amounts of pixels. First errors are named geometric errors, and second ones are named radiometric errors. Some of these errors are corrected in ground receiver stations, but the images should be finally assessed by users and corrected if necessary. Generally, corrections can be divided into two groups including geometric corrections and radiometric corrections (Lillesand and Kiefer, 1987; Jensen, 1996).
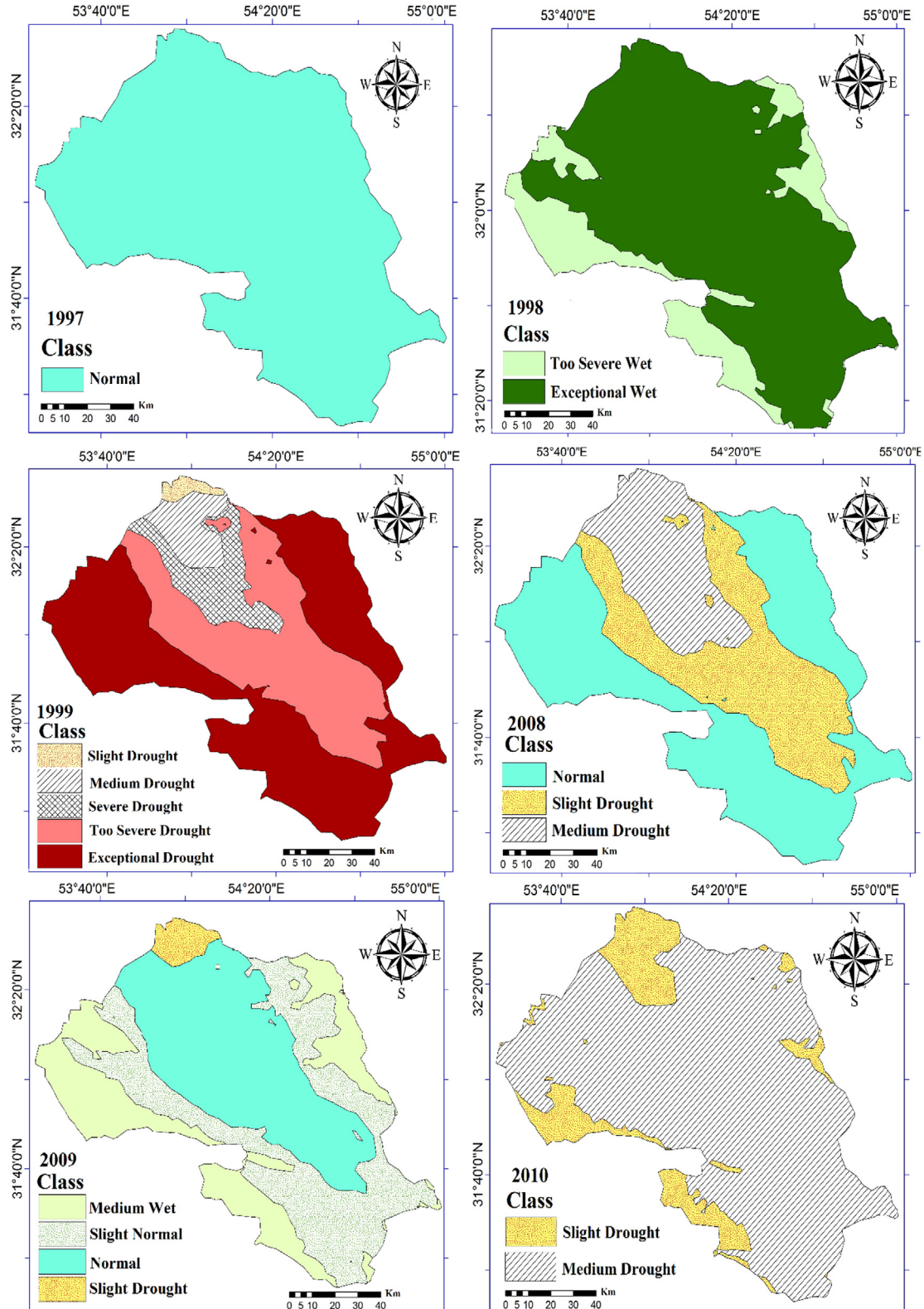

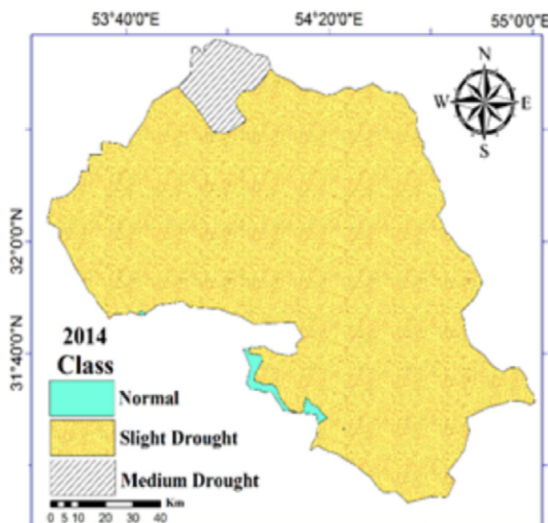**Fig. 4.** The zonation maps of the annual SPI (1997, 1998, 1999, 2008, 2009, 2010 and 2014).

Fig. 4 (*continued*)

2.2.3.1. *Geometric corrections.* Geometric correction is the first step for preparing satellite data. It can be done using ground control points, measured by GPS or maps that are corrected geometrically. Such maps could be satellite images of the region that are taken in past years, or air images taken from the region with high precision that are georeferenced utilizing ground region data. In that case, geographical position of each point in image is like its position on the ground. For geometrical correction in this research, applied images were accessed from an ASTER sensor image already corrected in geometrical terms. Also a numeric layer of roads and projections were made in image and the correction was completed using this layer (Moreno, 1999; Jensen, 1996; Schowengerdt, 2007).

2.2.3.2. *Radiometric corrections.* Radiometric corrections are employed for decreasing or deleting two types of main atmospheric and machine errors. Atmospheric errors are the result of atmosphere effect (absorption and scattering) on electromagnetic energy. Such correction takes place in two steps; the conversion of numeric value to the spectral radiance, and the conversion of

the spectral radiance to the spectral reflectance (Jensen, 1996; Schowengerdt, 2007).

By carrying out radiometric corrections, the effect of sunlight angle difference caused by the difference in time among the applied data is removed. Likewise, the spectral reflectance may correct the difference in spectral ranges that are rooted in various spectral bands (Xiajun and Lo, 2000).

2.2.4. Calculating and classifying NDVI

This is one of the most well-known herbal indices widely used in most researches and satellite studies for determining vegetation health and density which is explained through the Eq. (2) (Pôças et al., 2013):

$$NDVI = (NIR - RED)/(NIR + RED) \tag{2}$$

where:

NIR: the Reflection of the light in NIR bands
RED: the Reflection of the light in red band

In this formula, NIR is near infrared band and R is red band. Its domain is variable from −1 to +1. When vegetation is so good and dense, this index is close to +1 and it decreases in case of vegetation destruction. To obtain this index, we have used ILWIS and ENVI software.

After that, the index was classified in three classes including no vegetation, poor vegetation (pastures) and dense vegetation (farming lands and gardens) exploiting supervised classification after which the percentage area of each part was obtained. For assessing the authenticity of prepared maps, ground truth and random points which were taken from ground localization (positioning) set were used.

3. Results and discussion

The average of annual SPI was calculated through ArcGIS 9.3 and using maps of Yazd-Ardakan plain SPI in period of 1996–2015. The worst amount observed in drought indices in Yazd-Ardakan plain for annual SPI is −1.92 in 1999, and the annual SPI of 1996 with value of 2.4 was considered as the wettest year during study period of 1996–2015 (Table 1).
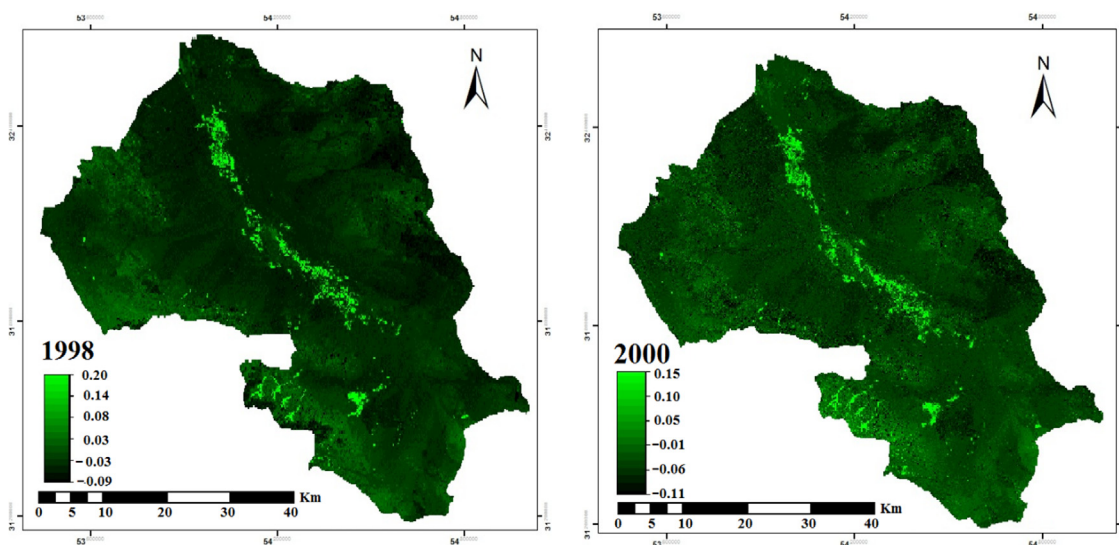

Fig. 5. The maps of NDVI (1998, 2000, 2009, 2010, 2011 and 2015).

Current averages of the SPI in different years are illustrated in Table 3. The most percentage of the area of dense vegetation and poor vegetation classes is related to 2010 and 1998 respectively, and the lowest percentage of the area for both classes is related to 2000.

According to Table 3, the worst amount of drought that occurred in period of 1996–2015 was related to year 1999, and the year 1998 considered as the wettest year among all years (Fig. 4). This might be because of annual insufficient precipitation in Iran (Zehtabian et al., 2010). The same result has been obtained by Bhat (2006) which showed 21.5% of India experienced inadequate annual rainfall and consequent severe drought was happened in most regions of the country.

Likewise, NDVI was calculated in order to highlight and reinforce the difference in spectral reflection between vegetation. For this purpose, TM and OLI sensors were used and the index map was classified into three groups including no vegetation, poor vegetation (pastures) and dense vegetation (farming lands around cities and cultured areas). Figs. 5 and 6 demonstrate samples of NDVI and classification maps of Ardakan-Yazd plain. The area and the percentage of each class are shown in Table 4.

Considering Fig. 6, the highest percentage of vegetation cover is related to 2010, and the lowest percentage refers to 2000. According to this, the most severe drought that has ever occurred

from 1996 to 2015 was in 1999; therefore, the lowest vegetation in Yazd-Ardakan plain has been in the next spring which is 2000.

The results of Table 4 indicate that cohesion of the area percentage of the poor vegetation class relating to the middle of the spring in each year. It shows a significant figures in 95% by the SPI of the previous year. There was correlation among the area of poor vegetation class in middle of spring and previous annual SPI at the significant level of 95%. In contract, no correlation was found between dense vegetation class areas in middle spring and previous amount of annual SPI. The reason is that, poor vegetation is related to pastures and margins of waterways that supply their own need for water from atmospheric rainfalls. This result corresponds to the researches accomplished by Ji and Peter (2003) and Jain et al. (2010).

Since the used satellite images are for late May and early June, drought index in the past year should be used in order to study the effect of drought on vegetation. Hence, areas percentage cohesion of the classes of dense and poor vegetations for 1998, 2000, 2009, 2010,2011 and 2015 were studied by the SPI in 1997, 1999, 2008, 2009, 2010 and 2014 in SPSS software by applying Pearson test. The results are provided in Table 5.

In Fig. 7, a diagram of vegetation areas percentage which is the total percentage of two classes of dense and poor vegetation is provided.
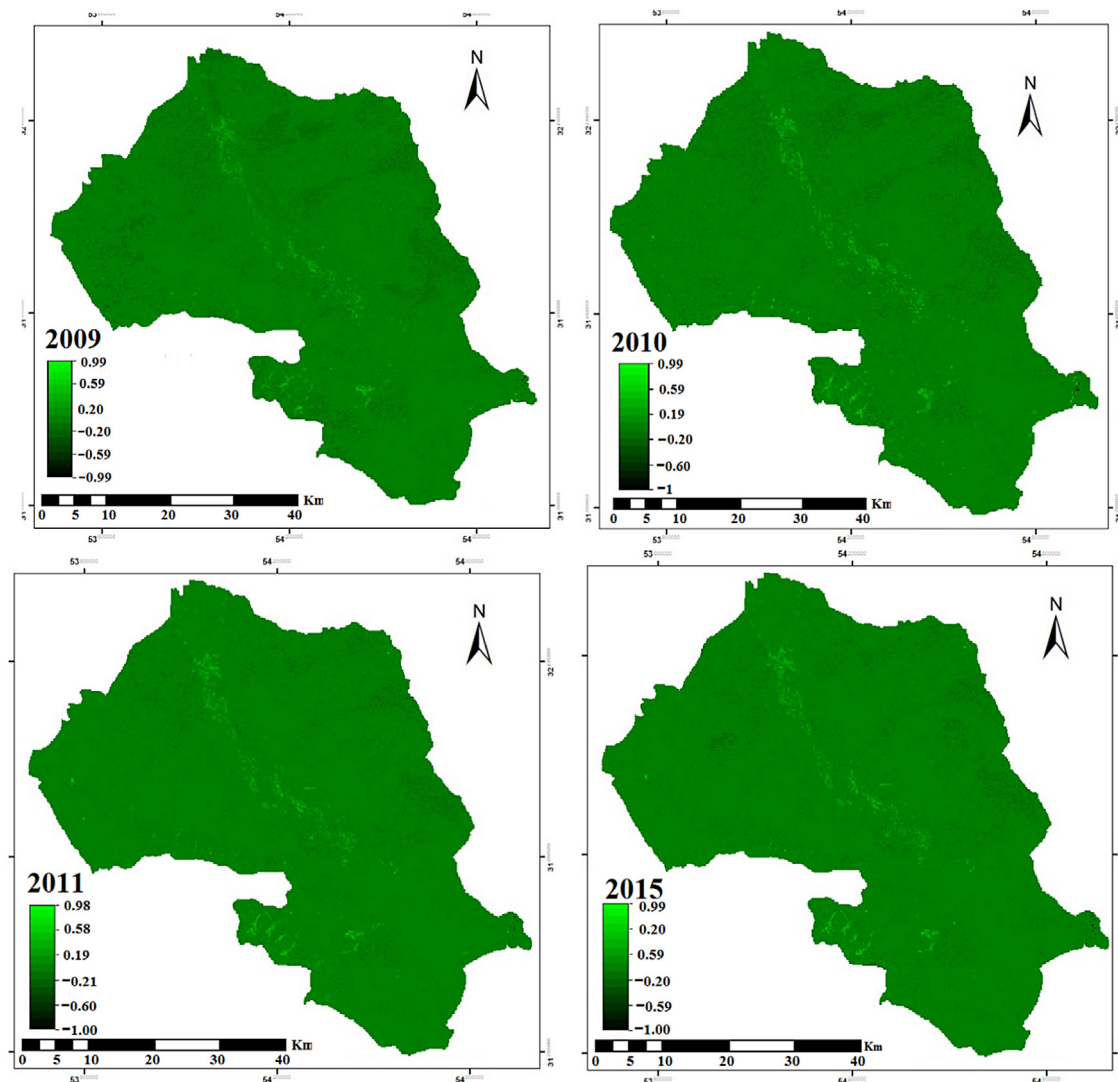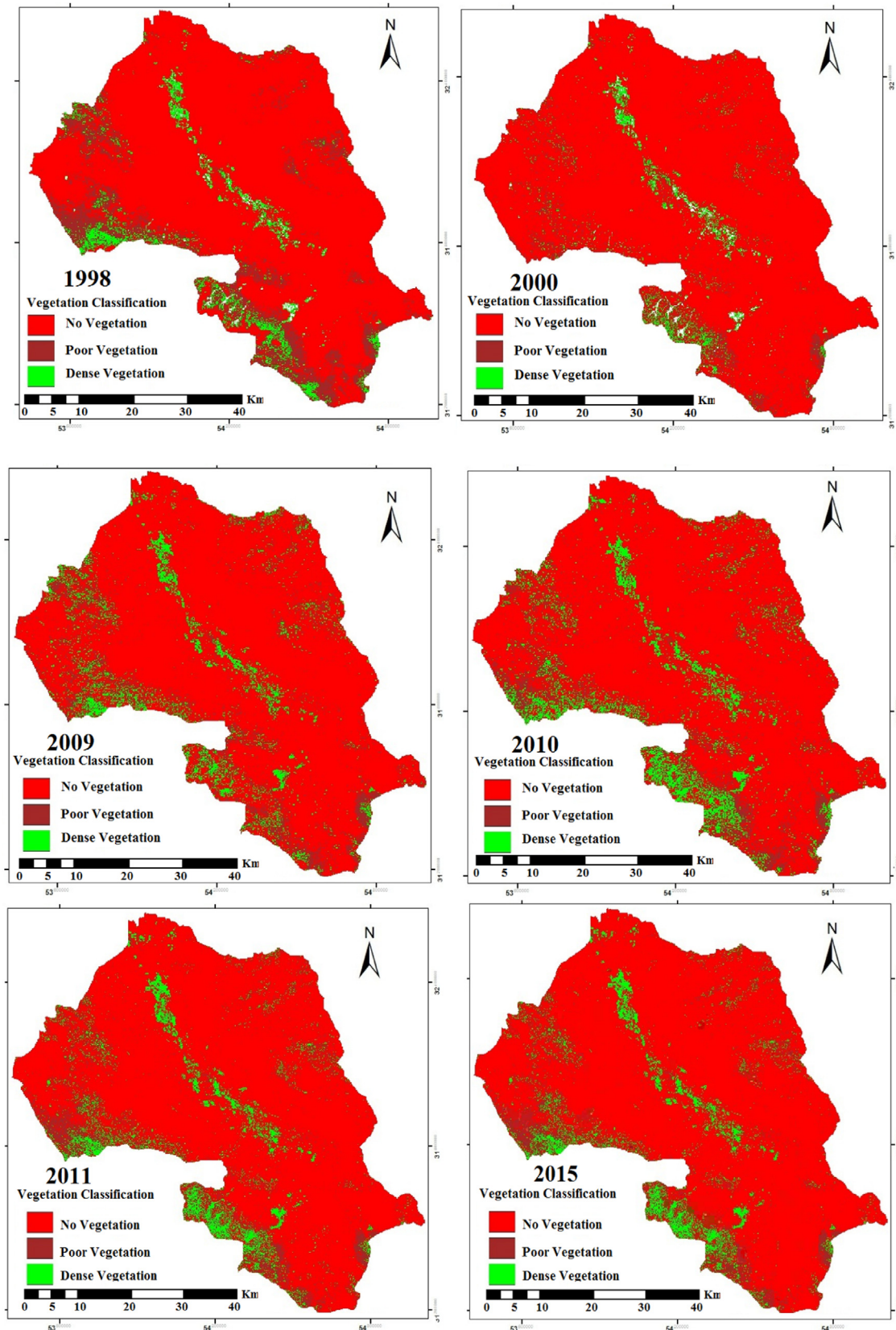

Fig. 5 (*continued*)

Fig. 6. The maps of vegetation classes (1998, 2000, 2009, 2010, 2011 and 2015).

4. Conclusion

This study analyzed the relationship between NDVI and SPI in Yazd-Ardakan Plain during the growing season. Based on the results there is a positive correlation between NDVI and SPI that means more rainfall lead to more vegetation cover. It can be said that NDVI and precipitation index have a strong correlation where water is a major limiting factor for plant growth.

Table 4
Results retrieved from satellite vegetation indices.

Classes Year	Dense vegetation		Poor vegetation		No vegetation	
	Area (km^2)	Percent	Area (km^2)	Percent	Area (km^2)	Percent
1998	581.89	4.98	1640.47	14.04	9461.97	80.98
2000	394.93	3.37	784.02	6.71	10505.38	89.91
2009	747.23	6.4	1297.67	11.11	9639.43	82.50
2010	944.97	8.09	1430.32	12.24	9309.04	79.67
2011	754.53	6.46	1259.11	10.78	9670.69	82.77
2015	690.05	5.94	1289.95	11.04	9700.33	83.02

Table 5
Results of cohesion of the percentage of areas for dense and poor vegetation classes with previous year.

		Poor vegetation	Dense vegetation
Pearson cohesion	SPI (previous year)	0.943	0.647
Sig. (2-tailed)		0.016	0.238
Number		5	5
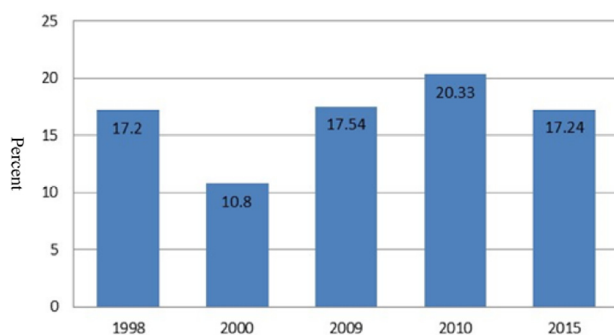
Fig. 7. Diagram of time changes on percent of vegetation area.

Any changes in amount of rainfalls affect vegetation classes immediately. However, dense vegetation class is related to farming lands, gardens around cities and villages. In those regions irrigating water is mostly supplied by deep and half-deep wells. The results also indicate that the highest correlations occurred during the middle of the growing season. This was likely due to sensitivity of plants to water availability during their growing season. This seasonal effect needs to be taken into account when regression techniques are used to quantify the NDVI and SPI relationship.

As a result, drought has not been able to cause a significant change in the area percentage of the dense vegetation. The temporal variations of NDVI anomaly are closely linked with SPI and have strong linear relationship with SPI. It should be noted that in the south west part and partly west of Yazd-Ardakan plain in which foothill Qanats provides vegetation water requirements, the area of the dense vegetation class is affected by drought. However, the relation between drought and the area of the dense vegetation class doesn't show any significant correlation. Regarding to define vegetation classes by NDVI maps, we can say there is a positive correlation between annual SPI (with delay) and the vegetation area of pastures as well as waterways margins.

There is no correlation between SPI and NDVI of farming lands and gardens with two months delay. The combination of remote sensing, NDVI vegetation data and climatic indexes are suitable for estimation of land cover changes (Zarei et al., 2016). It can be noted that NDVI can be a proper indicator of moisture condition and can be used as an important data source for detecting and monitoring drought in the arid and semiarid regions.

According to the results of this research, monitoring the drought needs simultaneous use of the climatic data and satellite images to obtain better results which is compatible to the research of Himanshu et al. (2015). Additionally, researches with more satellite images are needed to make mentioned facts about drought and its effects on vegetation more precise.

Conflict of interest

None declared.

References

Aboelghar, M., Arafat, S., Saleh, A., Naeem, S., Shirbeny, M., Belal, A., 2010. Retrieving leaf area index from SPOT4 satellite data. Egypt. J. Remote Sens. Space Sci. 13, 121–127.

Alshaikh, Y.A., 2015. Space application for drought assessment in Wadi-Dama (West Tabouk), KSA. Egypt. J. Remote Sens. Space Sci. 18, 43–53.

Barati, S., Rayegani, B., Saati, M., Sharifi, A., Nasri, M., 2011. Comparison the accuracies of different spectral indices for estimation of vegetation cover fraction in sparse vegetated areas. Egypt. J. Remote Sens. Space Sci. 14 (1), 49–56.

Bevan, S.L., Los, S.O., North, P.R.J., 2014. Response of vegetation to the 2003 European drought was mitigated by height. Biogeosciences 11, 2897–2908.

Bhat, G.S., 2006. The Indian drought of 2002—a sub-seasonal phenomenon? Q. J. R. Meteorol. Soc. 132, 2583–2602.

Bhuiyan, C., Singh, R.P., Kogan, F.N., 2006. Monitoring drought dynamics in the Aravalli region (India) using different indices based on ground and remote sensing data. Int. J. Appl. Earth Obs. Geoinf. 8, 289–302.

Boori, M.S., Voženílek, V., Choudhary, K., 2015. Land use/cover disturbance due to tourism in Jeseníky Mountain, Czech Republic: a remote sensing and GIS based approach. Egypt. J. Remote Sens. Space Sci. 18 (1), 17–26.

Brown, J.F., Wardlow, B.D., Tadesse, T., Hayes, M.J., Reed, B.C., 2008. The Vegetation Drought Response Index (VegDRI): a new integrated approach for monitoring drought stress in vegetation. GISci. Remote Sens. 45, 16–46.

Caccamo, J., Chisholm, L.A., Bradstock, R.A., Puotinen, M.L., 2011. Assessing the sensitivity of MODIS to monitor drought in high biomass ecosystems. Remote Sens. Environ. 115, 2626–2639.

Dutta, D., Arnab, K., Patel, N.R., Saha, S.K., Siddiqui, A.R., 2015. Assessment of agricultural drought in Rajasthan (India) using remote sensing derived Vegetation Condition Index (VCI) and Standardized Precipitation Index (SPI). Egypt. J. Remote Sens. Space Sci. 18, 53–63.

Goddard, S., Harms, S., Reichenbach, S., Tadesse, T., Waltman, W.J., 2003. Geospatial decision support for drought risk management. Communication of the ACM 46, 35–37.

Hadian, F., Hosseini, Z., Sayed Hassani, M., 2013. Monitoring of vegetation changes using rain data and satellite image of NOAA AVHRR in Kermanshah province, Iran. J. Rangeland 1, 46–62.

Himanshu, S.K., Singh, G., Kharola, N., 2015. Monitoring of drought using satellite data. Int. Res. J. Earth Sci. 3, 66–72.

Jain, C.F., Keshri, R., Gosvami, A., 2010. Application of meteorological and vegetation indices for evaluation of drought impact: a case study for Rajasthan, India. Nat. Hazards 54, 643–656.

Jensen, J., 1996. Introductory Digital Image Processing: A Remote Sensing Perspective. , pp. 128.

Ji, L., Peter, A.J., 2003. Assessing vegetation response to drought in the northern Great Plains using vegetation and drought indices. Remote Sens. Environ. 87, 85–98.

Lillesand, T.M., Kiefer, R.W., 1987. Remote Sensing and Image Interpretation. John Wiley & Sons, NY.

Mondal, S., Jeganathan, C., Sinha, N.K., Rajan, H., Roy, T., Kumar, P., 2014. Extracting seasonal cropping patterns using multitemporal vegetation indices from IRS LISS-III data in Muzaffarpur District of Bihar, India. Egypt. J. Remote Sens. Space Sci. 17, 123–134.

Montandon, L.M., Small, E.E., 2008. The impact of soil reflectance on the quantification of the green vegetation fraction from NDVI. Remote Sens. Environ. 112, 1835–1845.

Moreira, E.E., Coelho, C.A., Paulo, A.A., Pereira, L.S., Mexia, J.T., 2008. SPI-based drought category prediction using loglinear models. Hydrology 354, 116–130.

Moreno, J.F., 1999. Remote Sensing Geometric Corrections. Wiley Encyclopedia of Electrical and Electronics Engineering.

Pôças, I., Cunha, M., Pereira, L.S., Allen, R.G., 2013. Using remote sensing energy balance and evapotranspiration to characterize montane landscape vegetation with focus on grass and pasture lands. Int. J. Appl. Earth Obs. Geoinf. 21, 159–172.

Potop, V., Mozny, M., Soukup, J., 2012. Drought evolution at various time scales in the lowland regions and their impact on vegetable crops in the Czech Republic. Agric. Forest Meteorol. 156, 121–133.

Rahimzadeh, B., Darvishsefat, P., Khalili, A.A., Makhdoum, M.F., 2008. Using AVHRR-based vegetation indices for drought monitoring in the Northwest of Iran. J. Arid Environ. 72, 11086–11096.

Schowengerdt, R., 2007. Remote Sensing: Models and Methods for Image Processing. , pp. 337.

Shahabfar, A., Ghulam, A., Eitzinger, J., 2012. Drought monitoring in Iran using the perpendicular drought indices. Int. J. Appl. Earth Obs. Geoinf. 18, 119–127. http://dx.doi.org/10.1016/j.jag.2012.01.011.

Skandari, H., Borji, M., Khosravi, H., Mesbahzadeh, T., 2016. Desertification of forest, range and desert in Tehran province, affected by climate change. Solid Earth 7 (3), 905–915.

Unganai, L.S., Kogan, F.N., 1998. Drought monitoring and corn yield estimation in Southern Africa from AVHRR data. Remote Sens. Environ. 63, 219–232.

Water, W., Become, F., 2005. Managing Livestock During a Drought. University of Wisconsin-Extension, Cooperative Extension.

Xiajun, Y., Lo, C.P., 2000. Relative radiometric normalization performance for change detection from multi-date satellite images. Photogramm. Eng. Remote Sens. 66 (8), 967–980.

Yazdanpanah, H., Momeny, M., Dezfullian, H., Movahedy, S., Soleimanitabar, M., 2014. Drought monitoring of south of Khuzestan province, Iran using remote sensing and SPI. Geogr. Environ. Planning J. 54, 21–24.

Yingxin, G.Y., Brown, J.F., Verdin, J.P., Wardlow, B., 2007. A five-years analysis of MODIS NDVI and NDWI for grassland drought assessment over the central Great plains of the United States. Geophs. Res. Lett. 34, L06407.

Zarei, S., Khosravi, H., Nasiri, A., Dastorani, M., 2016. Using Landsat Thematic Mapper (TM) sensor to detect change in land surface temperature in relation to land use change in Yazd, Iran. Solid Earth 7, 1551–1564.

Zehtabian, G., Khosravi, H., Ghodsi, M., 2010. High Demand in a Land of Water Scarcity: Iran. Chapter 5. Springer, Netherlands, pp. 75–86.